Analysis of the Weld Seam Area of Magnetic Pulse Welded Aluminium-Steel-Sheet-Connections on its Suitability as a Sign of Quality

E.Schumacher[1*], S. Kümper[1], I. Kryukov[1], S. Böhm[1]

[1] Department for Cutting and Joining Manufacturing Processes, Institute for Production Technologies and Logistics, University of Kassel, Germany
*Corresponding author. Email: e.schumacher@uni-kassel.de

Abstract

This paper deals with the characterisation of the weld seam area of magnetic pulse welded aluminium-steel-sheet-connections for different material combinations and its suitability as a sign of quality. The goal of this work is to suggest a relationship between the weld seam area and the strength of the generated joint. Based on the results of this work, the weld seam area could be established as a basis of design and for dimensioning the magnetic pulse welded hybrid joints. To identify the correlation of the generated weld seam area with the maximum tensile force of the welded samples, several aluminium-steel-joints were welded and tested using tensile shear test. Thereafter, the weld seam area was measured and correlated to the maximum bearable tensile force of the joint. The tested material combinations were EN AW-1050A-H14 / S235JR and EN AW-6016-T6 / HCT780X. The results illustrate a positive linear correlation between the weld seam area of the joint and the maximum tensile force. At the same time further weld seam irregularities were identified which have to be considered for evaluating the suitability of the weld seam area as a sign of quality. Additionally, in order to prevent such irregularities or to ensure a good weld seam, the non-destructive testing method of active thermography is presented.

Keywords

Magnetic pulse welding, Aluminium, Steel

1 Introduction

Lightweight transport concepts are at present more strongly influenced than ever by the use of metallic hybrid structures. Legal requirements to reduce CO2-emmisions, rising energy costs as well as the growing social sustainability philosophy are the impulses driving manufacturers to increasingly integrate hybrid structures, especially made of aluminium and steel, in their products (Friedrich, 2013). Due to the metallurgical differences of these two metals, thermal joining processes (e.g. resistance spot welding) are not suitable to produce high-strength joints and thus mechanical joining (e.g. clinching, riveting) as well as adhesive joining processes despite their process-specific disadvantages dominate the field (Mori et al. 2013).

The magnetic pulse welding (MPW) offers enormous potential for solving such a welding task. It enables the realization of a metallurgical connection between dissimilar metals without the presence of a heat-affected zone. Thus, the welding process takes place below the melting temperatures of the materials, whereby no thermally induced microstructural changes occur and the mechanical properties remain unchanged (Zhang 2010). This advantage predestines MPW for producing high-strength aluminium-steel-connections.

Despite this potential and the intensified research activities since 1980s, MPW has not been able to gain acceptance for mass production. The industrial use is currently limited to smaller batch sizes in the automotive, aerospace and nuclear sector (Kapil and Sharma, 2015). In order to further qualify the MPW for industrial use and to increase the confidence of the manufacturers, it is necessary to offer alternative quality characteristics, which provide reliable information about the welding quality. These characteristics should ideally be non-destructively detectable in terms of continuous process and cost-efficient quality control. In the literature, efforts have already been made to establish such alternative quality characteristics with the primary focus on the size and geometric form of the weld seam. For example, Geyer et al. (2014) tried to quantify a correlation between the weld seam width and the bearable tensile force of the welded samples, but without success. A closer look on the study shows that only selected areas of the weld seam were taken into account and not the complete weld seam.

However, to meet the addressed demand, the investigation presented in this paper focuses on the one hand to quantify the relationship between the weld seam area and the bearable tensile force of the joint whereby, the complete weld seam is considered, and on the other hand to introduce the active thermography as a suitable non-destructive testing method.

2 Experimental Setup

2.1 Magnetic Pulse Welding

For the investigation the magnetic pulse system BlueWave PS48-16 in combination with the flat coil B80/10 (80 mm length, 10 mm width, 5 mm thickness) from PSTproducts GmbH was used. The pulse system has a maximum charging energy of 48 kJ, a maximum charging voltage of 16 kV and the flat coil can be operated until a peak current of 500 kA. During the welding process the current pulse provided by the pulse system will be released and conducted through the flat coil, which leads to the formation of radial magnetic field around the coil. This magnetic field, in turn, induces a current flow in the flyer sheet, which is positioned directly above the coil as shown in **Fig. 1**. According to the principle of mutual induction a second magnetic field of opposite direction to the primary magnetic field arises around the flyer sheet and the resulting electromagnetic force accelerates the flyer sheet across an adjusted acceleration distance (gap) towards the fixed target sheet. The impact velocity of the flyer sheet achieved in this process or more precisely the resulting contact pressure in the collision area of the joining partners causes them to weld together (Epechurin, 1974, Demchenko et al., 1992).

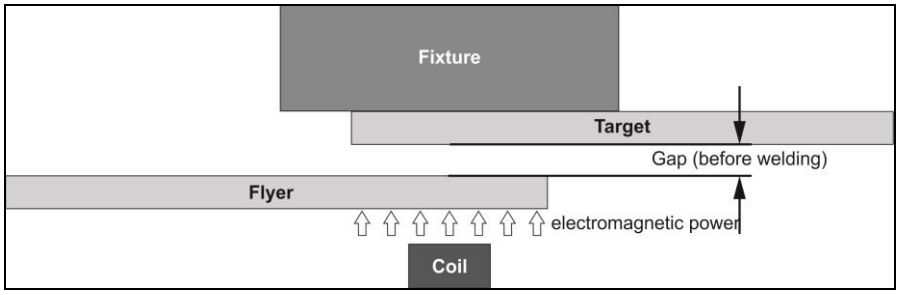

Figure 1: *Schematic representation of the MPW-process*

2.2 Materials and Welding Parameters

The experiments were carried out with four materials, whose tensile strength were determined in advance and are illustrated together with their thicknesses in **Table 1**. The size of all sheets were 100 x 40 mm².

Material	Thickness [mm]	Tensile strength [MPa]
EN AW-1050A-H14	1.5	110
EN AW-6016-T6	1.25	271
S235JR (1.0038)	1.5	344
HCT780X (1.0943)	1.5	824

Table 1: *Selected material constants*

Two material combinations were realised, whereby the joining partners were positioned parallel to each other with an overlap of 30 mm. The aluminium sheet always acted as flyer sheet. In order to reduce the scope of experiments for the main investigation, the minimum discharge current necessary for a successful weld was determined for all material combinations earlier by preliminary tests. Based on the achieved results, the settings of process parameters shown in **Table 2** were chosen for the main experiments.

Material combination	Average peak discharge current [kA]	Acceleration distance [mm]
EN AW-1050-H14 / S235JR	267 / 297 / 324 / 349	1 / 1.5 / 2
EN AW-6016-T6 / HCT780X	357 / 380 / 403 / 423	1 / 1.5 / 2

Table 2: *Realised Material combinations and used welding parameters*

The discharge current and the acceleration distance were varied according to a full factorial experimental design and three repetitions per test series or parameter set were performed. The discharge frequency averaged 19.8 kHz. To increase the reproducibility of the weld, the surfaces of the flyer and target sheets were laser ablated in the collision areas just prior to the welding operation.

2.3 Weld Seam and Correlation Analysis

The successfully welded samples were first subjected to a tensile test to determine the maximum tolerable tensile force. Unless the tested sample failed in the weaker base material (aluminium sheet) during the tensile test, the collided surface of the target sheet was then exposed to Weck's aluminium colour etchant to determine the weld seam area. An example of an etched target sheet surface is given in **Fig. 2**.

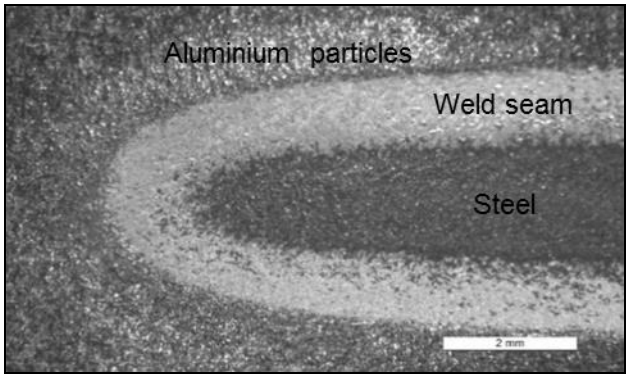

Figure 2: *Example of a successfully etched target sheet surface (HCT780X) in the collision area after the tensile test.*

This colour etchant, if used successfully, only attacks and dissolves aluminium. The resulting free surface then reacts with constituents of the etchant to form an insoluble compound, which again condenses as a yellow-greenish pigment on free surfaces. Intermetallic phases of aluminium and steel as well as steel itself are not affected during this process and retain their original colours. The result was a pronounced contrast which simplify the subsequent determination of the weld seam area under the optical microscope (Leica Z16APOA).

To quantify the relationship between the maximum tensile force and the weld seam area of the sample, the Pearson correlation coefficient was determined for each material combination. The normal distribution of both features necessary for this correlation analysis was proved by means of the Shapiro-Wilk-Test for all test series. The Shapiro-Wilk-Test works even for small sample sizes with a high quality of results.

2.4 Active Thermography

In order to introduce the active thermography as a suitable non-destructive testing method, additional samples from EN AW-6016-T6 / HCT780X with completely and partially formed weld seams were produced. The partially formed weld seams were generated by applying oil as a thin layer in the collisions area of the target sheet before welding. The samples were welded with a discharge current of 423 kA, an acceleration distance of 1.5 mm and the sample geometry, as shown in **Fig. 3** on the right. The doubling of the target sheet width to 80 mm served to reduce the influence of the edge effect in the area to be examined. The active thermography is a two-dimensional imaging measurement method in which the test specimen is impulsively stimulated by an inductor and a transient heat transport occurs. Material inhomogeneities, in this case, the weld seam, lead to local changes of the heat flow in the test specimen, which can be detected by a thermography camera positioned above the specimen, as shown in **Fig 3** on the left.

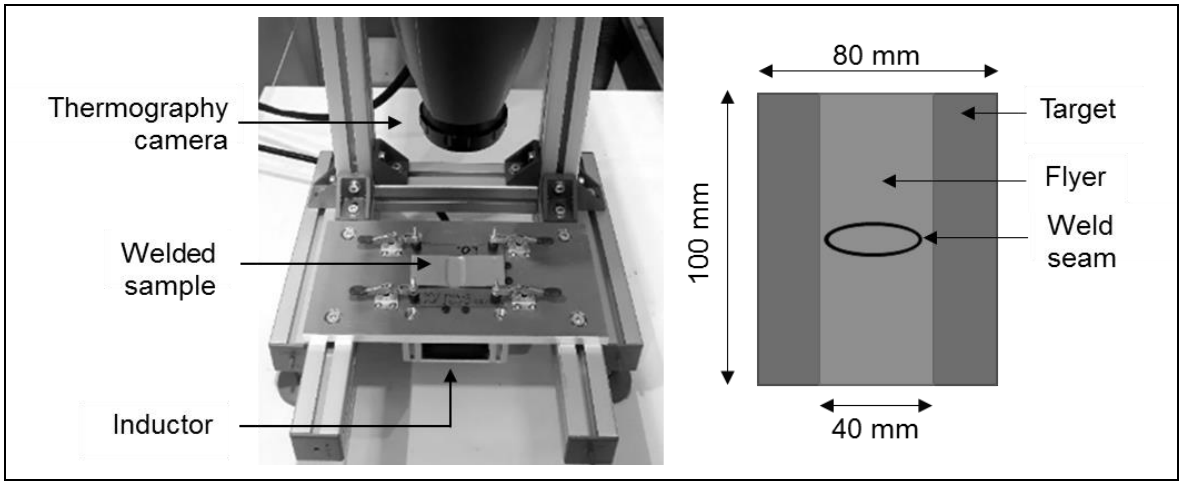

Figure 3: *Active thermography. Left: Test setup. Right: Sample geometry*

The induction-based thermal stimulation of the sample was carried out with an induction frequency of 8 kHz over a pulse duration of 0.1 s and a pulse width modulation of 375 ‰. The occurring heat radiation was detected and evaluated with the thermography system SC5600-M from FLIR Systems GmbH in the infrared range.

3 Results

Fig. 4 shows the achieved tensile forces of the samples depending on the applied discharge current and the acceleration distance for both material combinations.

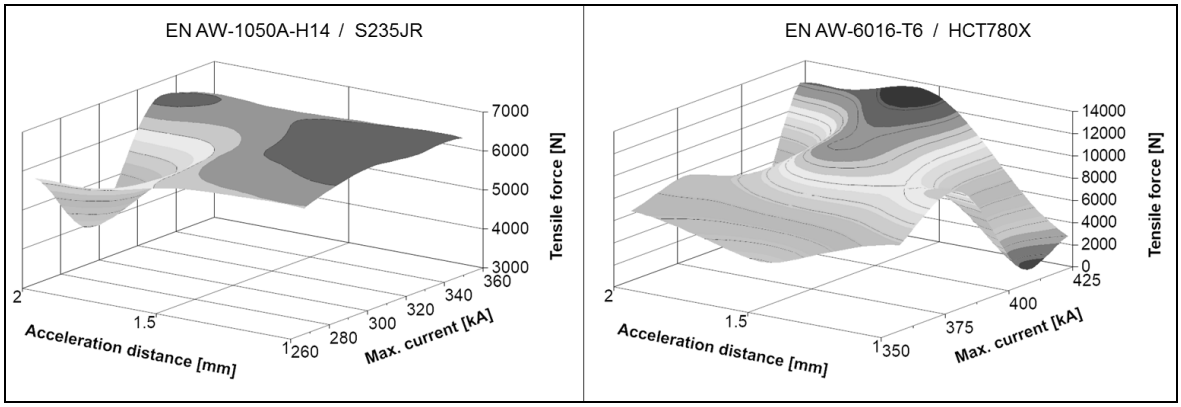

Figure 4: *Tensile force depending on the discharge current and acceleration distance. Left: EN AW-1050A-H14 / S235JR. Right: EN AW-6016-T6 / HCT780X*

For the material combination EN AW-1050A-H14 / S235JR (**Fig. 4** left) the lowest applied discharge current of 267 kA was enough to achieve considerably high average tensile force of 5800 N for all acceleration distances. With an increasing current, the series welded with 1 mm and 1.5 mm overcame the limit of 6400 N, such that with a current of 297 kA already few and with a current of 324 kA all samples of these series failed in the weaker base material (EN AW-1050A-H14) during the tensile test. This relation could not be observed for the series welded with an acceleration distance of 2 mm. In this case, the negative influence of an increased acceleration distance was clearly identifiable. The samples welded with 297 kA had the lowest tensile force values of around 4000 N. Higher tensile forces were achieved again with a current of 324 kA, whereby most of the samples failed in the weld seam, even with a current of 349 kA.

A slightly different evolution was observed for the material combination EN AW-6016-T6 / HCT780X (**Fig. 4** right). Here, the series welded with an acceleration distance of 1.5 mm showed the best results. The tensile force gradually rose with an increased discharge current to a maximum of 13700 N. Although, all samples failed during the tensile test in the weld seam but showed significant necking in EN AW-6016-T6. The series welded with an acceleartion distance of 1 mm and 2 mm also showed increased tensile force in the beginning with an increasing discharge current but then rapidly fell to

2000 N at 403 kA. With current levels of 432 kA, only the samples welded with 2 mm reached higher tensile forces again.

The comparison of the achieved tensile forces with the determined weld seam areas is shown for the material combination EN AW-6016-T6 / HCT780X in **Fig. 5** on the left. The illustrated distribution indicated a linear relationship between these two characteristics. This was also confirmed by a calculated Pearson correlation coefficient of 0.93. Thus, a strong linear relationship could be quantified between the tensile force and the weld seam area. The Shapiro-Wilk-Test used to prove the normal distribution was positive for both characteristics and all test series (**Fig. 5**, on the right).

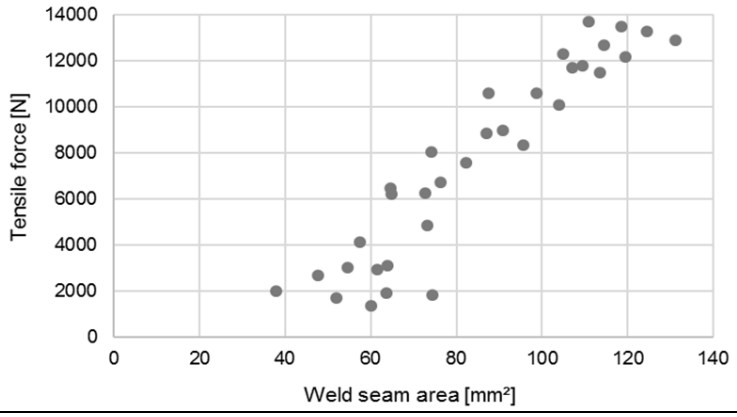

Shapiro-Wilk-Test W_{krit} = 0,767 α = 0,05			
Test series / Parameter set		Test results	
Dis. current [kA]	Acc. distance [mm]	Tensile force	Weld seam area
357	1,5	0,78	0.93
357	2	0,79	0,84
380	1	0,97	0,98
380	1,5	0.98	0,99
380	2	0.97	0.97
403	1	0.96	0,99
403	1,5	0.97	0,99
403	2	0.90	0,94
423	1	0.97	0,92
423	1,5	0.99	0,99
423	2	0.94	0,95

Figure 5: *EN AW-6016-T6 / HCT780X. Left: Comparison of tensile forces and weld seam areas. Right: Results of the Shapiro-Wilk-Test.*

The material combination EN AW-1050A-H14 / S235JR showed a different result. In this case, the correlation coefficient was only 0.73, which represents a medium linear relationship. The Shapiro Wilk test was again positive for all test series of this material combination.

An explanation for the lower correlation coefficient of the material combination EN AW-1050A-H14 / S235JR was provided by the evaluation of the images of the etched target surface in the collision area. It was found that the samples with a completed weld seam and a constant width of the elliptical ring, as shown in **Fig. 6** (top), were exclusively characterized by high tensile forces and simultaneously high weld seam areas. Samples with an incomplete weld seam or especially with an inconstant width of the elliptical ring (weld seam width) showed comparable large weld seam areas but achieved considerably lower tensile forces as shown in **Fig. 6** (middle and bottom), whereby this deviation is particularly pronounced with a strongly varying width of the weld seam. These results are in good agreement to those of Psyk et al. (2017), which illustrates that an increasing weld seam width, in this case the width of a linear formed weld seamed caused by the comparatively strong reduced overlap of 4 mm, leads to an increase in tensile force bearable by the welded sample.

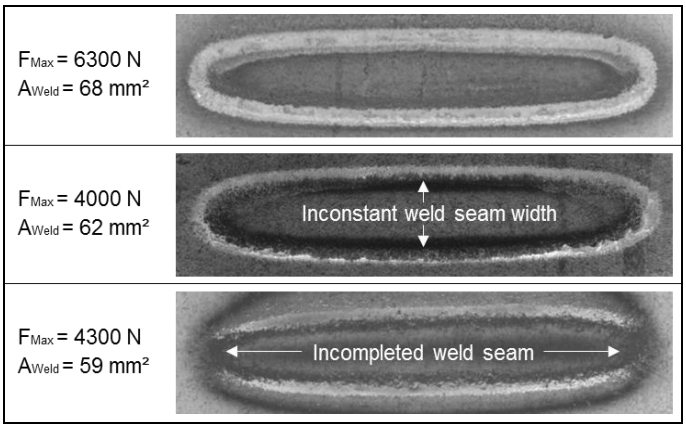

Figure 6: *Images of colour-etched target sheets (S235JR) in the collisions area. Top: Completely and with constant width formed weld seam. Middle: Completely, but with inconstant width formed weld seam. Bottom: Incompletely formed weld seam.*

Thus, the lower correlation coefficient could be due to the fact, that in the case of a strong variation of the weld seam width, areas with a comparable small width are exposed to local stress peaks, which exceeded the local tensile strength of those areas and finally initiate the complete failure of the weld seam. Such weld seam irregularities, have to be regarded as very critical and to be avoided in all circumstances.

The additional tests carried out with the active thermography showed that this non-destructive test method is ideally suited to prevent such irregularities or to guarantee a completely formed weld seam. The results are shown in **Fig. 7**.

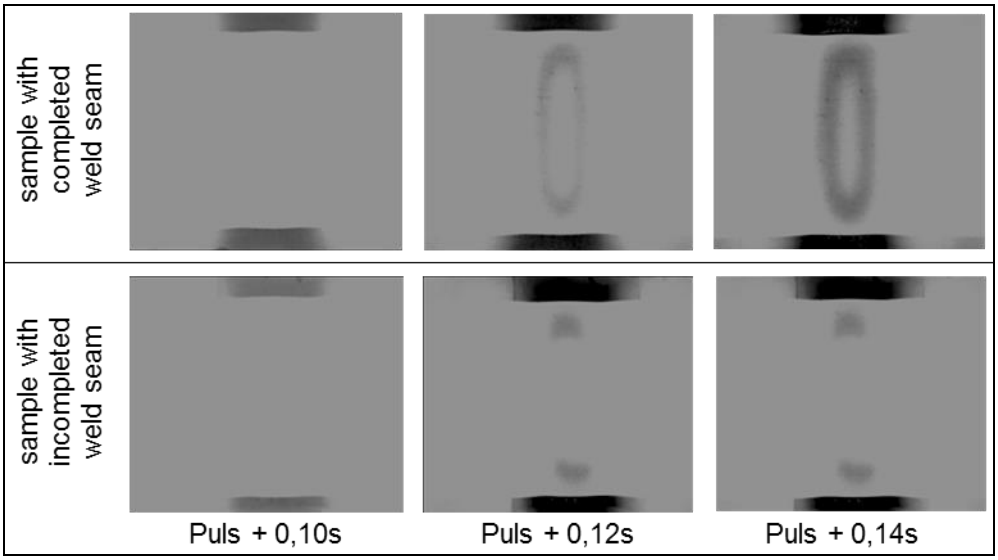

Figure 7: *Inverted thermographic images during the induction-based thermal stimulation. Above: Sample with completed weld seam. Below: Sample with incompleted weld seam caused by a thin oil layer.*

As illustrated, the thermal radiation detected by the thermography camera, which in turn was caused by the local changes of the heat flow in the test specimen during induction-based thermal stimulation, enabled a visualization of the welded areas. The completely formed weld seam as well as the partially formed weld seam caused by the thin oil film in the collision area were easily identifiable within a very short time period.

4 Conclusion and Outlook on Future Work

The presented investigation shows that the weld seam area is suitable as a sign of quality, if certain restrictions are taken into account. The determined Pearson correlation coefficient of 0.93 for the material combination EN AW-6016-T6 / HCT780X as well as the coefficient of 0.73 for the material combination EN AW-1050A-H14 / S235JR supports the weld seam area as a sign of quality but simultaneously illustrates that the linear correlation between the weld seam area and bearable tensile force of the joint depends on the realised material combination. In comparison with the available literature, it could be inferred that this correlation is qualitatively also valid for other material combinations (aluminium to copper, aluminium to aluminium, aluminium to stainless steel) or even different welding setups (Psyk et al. 2017). Finally, in the case of a ring-elliptical shaped seam it has to be considered, that the weld seam area only provides reliable information on the tensile strength of the sample after the exclusion of certain strength-reducing irregularities, such as an incompletely formed weld seam and especially an inconsistent weld seam width.

Further restrictions, which were not considered in this investigation but have to be taken into account in the future work, are the presence of brittle intermetallic phases of aluminium, their layer thickness as well as their well-known strength-reducing effect (Lee et al., 2007, Mary et al., 2007). Further investigations have to be performed to obtain a more comprehensive and precise overview about all known characteristics/irregularities and their strength-reducing effects.

The desired introduction of the active thermography as a suitable non-destructive testing method was successfully implemented. The presented method enabled the visualization of the welded areas without destroying the test specimen. Future work will focus on the development of the algorithms to determine the real weld seam size based on the recorded thermographic images.

Acknowledgments

This paper is based on the results acquired in the subproject A9 of the priority program 1640 (Joining by plastic deformation). The authors would like to thank the German Research Foundation (DFG) for the financial support.

References

Demchenko, V.F., Ryabchenco, V.R., Bocharikov, I.V., Zvoliskil, I.V., 1992. *Calculating the collision speed of Al Shells in magnetic pulse welding.* Paton Welding Journal 4 (6), pp. 23-25.

Epechurin, V.P., 1974. *Properties of bimetal joints by magnetic pulse welding.* Weld Prod 21 (5), pp. 4-12.

Friedrich, H. E., 2013. *Leichtbau in der Fahrzeugtechnik*. Springer Vieweg Verlag, Stuttgart.

Geyer, M., Rebensdorf, A., Böhm, S., 2014. *Influence of the Boundary Layer in Magnetic Pulse Sheet Welds of Aluminium to Steel.* In: Huh, H. (Eds.), Tekkaya, A.E., High Speed Forming 2014, Proceedings of the 6th International Conference, Daejeon, Korea, pp. 51-60.

Kapil, A., Sharma, A., 2015. *Magnetic pulse welding: An efficient and environmentally friendly multi-material joining technique.* Journal of Cleaner Production 100, pp. 35–58

Lee, K.J., Kumai, S., Arai, T., Aizawa, T., 2007. *Interfacial microstructure and strength of steel/aluminium alloy lap joint fabricated by magnetic pressure seam welding.* Materials Science and Engineering 471 (1-2), pp. 95-101

Marja, M., Rathod, M.J., Marya, S., Kutsuna, M., Priem, D., 2007. *Steel-to-Aluminum Joining by Control of Interface Microstructures - Laser-Roll Bonding and Magnetic Pulse Welding* -. Materials Science Forum, Vol. 539-543, pp. 4013-4018.

Mori, K., Bay, N., Fratini, L., Fabrizio, M., Tekkaya, A.E., 2013. *Joining by plastic deformation.* CIRP Annals – Manufacturing Technology 62 (2), pp. 673-694.

Psyk, V., Scheffler, C., Linnemann, M., Landgrebe, D., 2017. *Process analysis for magnetic pulse welding of similar and dissimilar material sheet metal joints*. Procedia Engineering 207 (2017), pp. 353-358.

Zhang, Y., 2010. *Investigation of magnetic pulse welding on lap joint of similar and dissimilar materials.* Ph. D. Thesis. The Ohio State University.